 SL, vol.3, no.1, pp.37-57, 2010

Multiple Interacting and Coalescing Semi-Elliptical Surface Cracks in Fatigue-Part-I: Finite Element Analysis

S. K. Patel[1], B. Dattaguru[2] and K. Ramachandra[1]

Abstract: Damage tolerance analysis is essential for evaluating life extension of aged structures which are in service beyond originally stipulated life. The major issue for such an analysis for aged aero-engines is the effect of multiple three-dimensional flaws on the structural integrity. In this paper, an improved modified virtual crack closure integral technique is applied to investigate the interaction of twin coplanar semi-elliptical cracks in a finite body under both tension and bending. The specific configuration analysed and presented here is two semi-elliptical surface cracks for combinations of various aspect ratios, thickness ratios and combination of interspacing. The interaction effects are studied for both interacting and coalescing phases as observed to occur during the growth of multiple surface cracks under fatigue load. Empirical equations are formulated to estimate interaction factors which could be used in simulation of fatigue crack growth of three-dimensional multi-site damage.

1 Introduction

In order to use the damage tolerance approach in high technology structures, the primary requirement is the ability to accurately estimate fatigue life or residual life in the presence of cracks. Fatigue damage in thick structural parts such as those in aero-engines normally manifests in the form of surface cracks which may be through, part through or a cluster of such cracks. For reliable prediction of fatigue life in the presence of such cracks, it is essential to develop methods for accurate estimation of stress intensity factors along the crack front and methods to develop crack shape at various stages of growth due to fatigue loading. For structures which are being newly designed and built, the primary issue will be damage tolerance in the presence of cracks which could be missed during non-destructive testing. On the other hand, for structures which are in service beyond their originally stipulated

[1] Gas Turbine Research Establishment, Bangalore
[2] Department of Aerospace Engineering, Jain University, Bangalore (formerly at) Indian Institute of Science, Bangalore

life (aged structures) a primary concern would be damage tolerance in the presence of multi-site damage. An understanding of fracture behavior of inter-acting multiple cracks is required to carry out life extension of such structures. These cracks may interact depending upon their geometry, spatial location, structure geometry and mode of loading. Interaction between multiple cracks becomes significant when they are nearby and it is important to evaluate these effects to accurately estimate the life of various components.

There are very few solutions for multiple semi-elliptical surface cracks in literature. Murakami et al [Murakami and Nemat-Nasser (1982)] and Isida [Isida, Yoshida and Naguch (1990)] have used body force method to estimate stress intensity factors for two equal semi-elliptical surface cracks in a semi-infinite body. O'Donoghue et al [Donoghue, Nishioka and Atluri (1986)] used an alternating method in conjunction with finite element method for multiple surface cracks in pressure vessels. These studies were limited to interaction phase of multiple fatigue crack growth of surface cracks. Kishimoto et al [Kishimoto, Soboyejo, Smith and Knott (1989)] have published results showing the variation of stress intensity factor around profiles of typical coalescing cracks. Soboyejo et al. [Soboyejo, Knott, Walse and Cropper (1990)] although presented interaction factors for both interacting and coalescing phases but only for limited cases (aspect ratios a/c=0.83 and 0.67) using strain energy difference method.

During 80's modified virtual crack closure integral (MVCCI) technique [Rybicki and Kanninen (1977); Buchholz (1984); Badari Narayana, Dattaguru, Ramamurthy and Vijaykumar (1994); Narayana, George, Dattaguru, Ramamurthy and Vijaykumar (1994)] was developed extensively for evaluation of Strain Energy Release Rate (SERR) components in two- dimensional problems with cracks. For three-dimensional cracks for estimation of strain energy release rates has been improved by Patel [Patel (2000)] to deal with curved crack front and unequal elements across the crack front. The accuracy of this method was demonstrated for certain benchmark surface flaw problems. Here, this improved MVCCI is used to study interaction between three-dimensional cracks in a multiple surface crack situation in a finite body. These are coplanar semi-elliptical cracks subjected to uniform tension and pure bending. Many of these developments are reviewed by Kruger [Kruger (2004)].

There were other attempts to evaluate SIF along the crack front by various workers. Chahardehi et al [Chahardehi and Brennan and Han (2010)] developed an RMS SIF estimation method to avoid the problems of surface point where the stress state changes from three-dimensional to biaxial. Xiao and Yan [Xiao and Yan (2007)] used FRANC3D software developed by Cornell University to arrive at SIF distribution along the crack front. Lin and Smith [Lin and Smith (1999)] in their two part

paper used the Newman and Raju [Newman Jr. and Raju (1979)] method of 2-point plus semi-elliptical growth to develop the crack front as it grows. The work which is close to the present work is by Kamaya [Kamaya (2008)] and in a two part paper he developed the crack growth shape in interacting surface cracks and applied it to map the crack growth in the case of two parallel cracks.

In this first part of the paper finite element analysis of these configurations is presented along with numerical studies in which stress intensity factors are presented in terms of basic geometric parameters, parametric angle and separation between the cracks. The interaction effects are studied for both interacting and coalescing phases as observed to occur in the growth of multiple surface cracks. This is a comprehensive study combining both interacting and coalescing phases starting with two cracks in the close neighborhood and taking them through the stage of merging into a single crack. Extensive numerical work is performed to study the effects of various parameters such as aspect ratio, thickness ratio and interspacing on the interaction factor. Using these solutions, empirical equations are formulated to estimate interaction factors. This facilitated the development of a simple semi-analytical method to study fatigue crack growth of multiple cracks.

2 Methodology

The modified virtual crack closure integral technique [Badari Narayana, Dattaguru, Ramamurthy and Vijaykumar (1994); Narayana, George, Dattaguru, Ramamurthy, and Vijaykumar (1994)] with curvature correction [Patel (2000)] in conjunction with the finite element method is used in estimating mode-I strain energy release rate and stress intensity factor for three-dimensional interacting cracks. In this technique for a three-dimensional solid, the work required to close an infinitesimal area of virtual crack extension is expressed in terms of nodal forces and displacements in the elements forming the crack front. Consider the finite element idealisation of surface crack configuration with the eight noded conventional brick elements along the crack front as shown in Fig.1, the SERR for G_I(p) is given by [Badari Narayana, Dattaguru, Ramamurthy and Vijaykumar (1994)]

$$G_I(p) = \frac{1}{2\Delta A_k}\left[4J_0C_{11} + 4J_1C_{12} + 4J_2C_{13}\right] \tag{1}$$

where

$$C_{11} = a_0b_0 + a_1b_1/3 + a_2b_2/3 + a_3b_3/9$$

$$C_{12} = a_1b_1 + a_1b_0/3 + a_2b_3/3 + a_3b_2/9$$

$$C_{13} = a_2 b_2 + a_1 b_3/3 + a_2 b_0/3 + a_3 b_1/9$$

and the Jacobian $|J| = J_0 + J_1\xi + J_2\eta$ where ξ and η are natural coordinates.

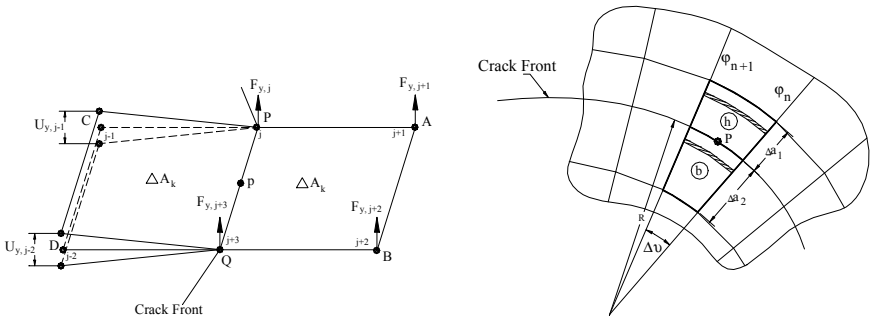

Figure 1: (a): Nodal displacements and forces on a face of kth eight noded brick element at crack front, (b): Schematic of finite element mesh at crack front

At this stage ΔA_k can be assumed as the area of element 'b' behind the crack front (Fig. 1b). For a sufficiently small element size, one could use the area of element as virtual crack extension area. The coefficients a_i (i=0,1,2,3) can be determined from the nodal values of displacements (Fig. 1) as follows

$$\begin{Bmatrix} a_0 \\ a_1 \\ a_2 \\ a_3 \end{Bmatrix} = \frac{1}{4} \begin{bmatrix} 1 & 1 & 1 & 1 \\ -1 & 1 & 1 & -1 \\ -1 & -1 & 1 & 1 \\ 1 & -1 & 1 & -1 \end{bmatrix} \begin{Bmatrix} U_{y,j-1} \\ U_{y,j} \\ U_{y,j+3} \\ U_{y,j-2} \end{Bmatrix} \tag{2}$$

The coefficient b_i (i=0,1,2,3) can be obtained from the equivalent nodal forces as

$$\begin{Bmatrix} b_0 \\ b_1 \\ b_2 \\ b_3 \end{Bmatrix} = 4 \begin{bmatrix} J_0 & J_1/3 & J_2/3 & 0 \\ J_1/3 & J_0/3 & 0 & J_2/9 \\ J_2/3 & 0 & J_0/3 & J_1/9 \\ 0 & J_2/9 & J_1/9 & J_0/9 \end{bmatrix}^{-1} \begin{bmatrix} 1 & 1 & 1 & 1 \\ -1 & 1 & 1 & -1 \\ -1 & -1 & 1 & 1 \\ 1 & -1 & 1 & -1 \end{bmatrix} \begin{Bmatrix} (F_h)_{y,j} \\ (F_h)_{y,j+1} \\ (F_h)_{y,j+2} \\ (F_h)_{y,j+3} \end{Bmatrix} \tag{3}$$

F_h refers to forces obtained from the element 'h' (Fig. 1b)

Due to curved crack front, it is convenient to use elements of unequal size across the crack front. A correction factor for this case was presented by Patel [Patel (2000)]. The "curvature and area correction factor" to be multiplied in MVCCI force coefficient matrix in eq. (3) is given by

$$(F_b)_{y,j+i} = (F_h)_{y,j+i} \left[\sqrt{\frac{\Delta a_2}{\Delta a_1}} \left\{ \frac{1 - \frac{1}{3}\frac{\Delta a_2}{R}}{1 + \frac{1}{3}\frac{\Delta a_1}{R}} \right\} \right] \tag{4}$$

where i assumes values equal to 0, 1, 2 and 3.

3 Results and discussions

The presence of multiple cracks is quite common in engineering structures. Under fatigue loads these cracks may initially grow independently based on their geometries and distance between them. As the cracks come closer they start interacting and the crack propagation rates increase and eventually cracks linkup to behave as coalescing crack prior to formation of a single dominant crack. This process of fatigue crack growth of multiple cracks can be divided into four phases-

1. Isolation period (cracks are sufficiently far away such that interaction factor is one).
2. Interaction period (when cracks approach each other and are close).
3. Coalescence period (when cracks coalesce).
4. Dominant single crack growth period (the two cracks merge into a single crack).

Crack growth of individual cracks during the isolation period or that of dominant crack can be predicted following usual procedure. But during the interaction and coalescence periods the adjacent cracks influence growth of each other depending on the change in their stress intensity factors. These cracks may interact depending upon their geometry, spatial location, structure geometry and mode of loading. These effects are usually represented by interaction factors. The estimation of interaction factor for interacting and coalescing multiple surface cracks is required to carry out accurate life prediction of components in presence of three-dimensional multiple cracks. Here, improved MVCCI[Patel (2000)] (with area and curvature corrections) is used to handle curvature and unequal areas across the crack front of interacting and coalescing equal semi-elliptical cracks in a finite body cracks and a comprehensive stress intensity factor solution is provided for both of them.

3.0.1 Multiple interacting surface cracks

In the present numerical study, the interaction of twin coplanar semi-elliptical cracks in a finite body under uniform tension and bending has been studied. The geometric parameters of interacting surface cracks are shown in Fig. 2. The specific configurations analysed are two identical semi-elliptical cracks of aspect ratio a/c=0.25, 0.50, 0.75 for various combinations of interspacing (t_s) in a plate of crack-depth ratio a/t=0.25, 0.50, 0.75 and crack-width ratio of 0.2. One of the finite element models used for estimation of stress intensity factor is shown in Fig. 3(a)-(b). The model consists of 7120 nodes and 5876 linear eight-noded elements and is only for half the configuration considering symmetry of the case of equal intersecting cracks.

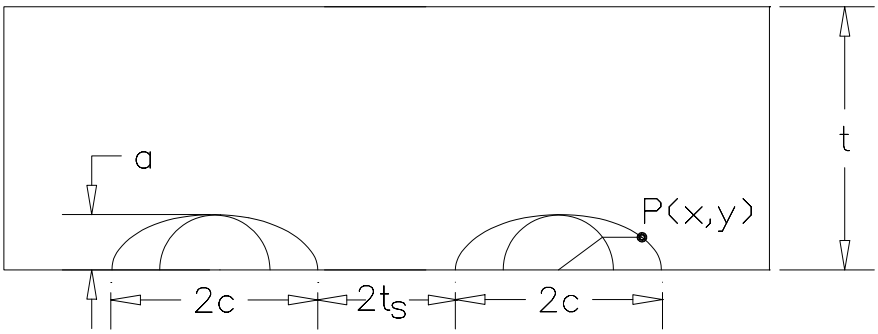

Figure 2: Geometric parameters of interacting surface cracks

The SIF solutions of single crack are also evaluated to enable the estimation of interaction factor for the case of multiple cracks. Some of these solutions for single cracks (a/c=0.25, a/t=0.25-0.75) are shown in Fig. 4. In order to compare the accuracy of present solution Newman-Raju [Newman Jr. and Raju (1981)] solutions are also plotted in Fig. 4. The close agreement between present results and Newman-Raju solutions demonstrates the reliability of present technique and finite element models.

The stress intensity factors for multiple semi-elliptical surface cracks for various geometric parameters a/c, a/t and t_s/c were estimated with MVCCI. The normalised stress intensity factor ($K_I/\frac{\sigma\sqrt{\pi a}}{Q}$) variation with parametric angle for various values of interspacing (keeping a/c=0.5, a/t=0.25) is shown in Fig. 5(a) and Fig. 5(b) along with stress intensity factor for a single crack of same geometric parameters subjected to tension load and bending loads respectively. It is observed that the

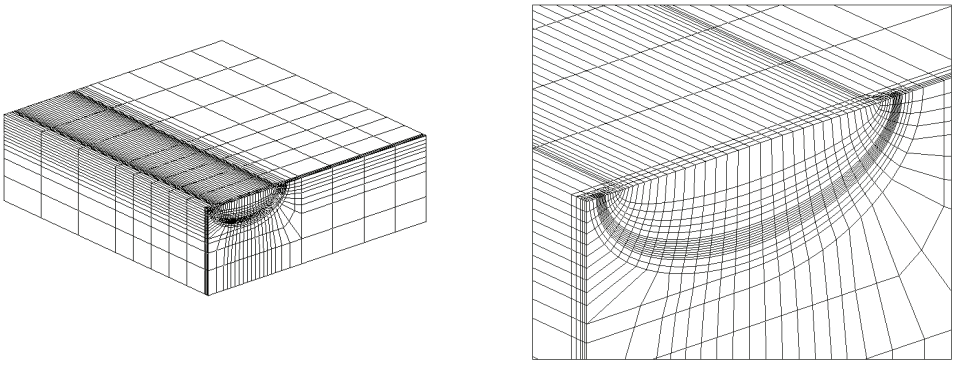

(a) (b)

Figure 3: (a): Finite element model (only half symmetric) of interacting crack (a/c=0.5, a/t=0.25, t_s/c=0.1). (b). Mesh details at crack front

presence of second crack affects significantly the stress intensity factor in the region approximately 0-30 degrees (150˚-180˚ in Fig. 5a) from the interacting plane. A marginal increase in stress intensity factor is also observed along the entire crack front compared to single crack.

The interaction between cracks is represented by interaction factor. Here the interaction factor, γ, is defined as the ratio of stress intensity factor at a point along the crack front in the presence of another crack in the neighbourhood to that in the absence of another crack in the neighbourhood. The solution in absence of the second crack is obtained from Fig. 4. The interaction factors as a function of crack interspacing (t_s/c) and aspect ratio (a/c) at the plate surface (φ=180˚) under tension load are obtained by MVCCI method and are plotted in Fig. 6. The results indicate that the interaction effect is significant when the cracks are separated by a small distance. As the distance between two cracks is approximately equal to the length of a crack (t_s/c=0.5), the interaction factor is less than 1.05. It is also observed that the interaction factor increases with increase in aspect ratio (a/c) but the effect is relatively less compared to crack interspacing. It is seen that the interaction factors are only marginally different between tension and bending loading (Fig. 7).

The interaction factors at parametric angle φ=0˚, 90˚ and 180˚ for the interacting semi-elliptical surface cracks under tension loading are listed in Tab. 1. It is seen from the table that the effect of aspect ratio on the interaction factor is more pronounced at small values of interspacing (t_s/c).

Table 1: Typical interaction factors, γ, at elliptical angle φ=0°, 90° and 180° as functions of normalised interspacing (t_s/c), aspect ratio (a/c) and thickness ratio (a/t) for two equal symmetric cracks in a finite plate under tension loading.

		Interaction Factor, γ									
a/c◇			0.25			0.50			0.75		
a/t	t_s/c	Angle	0°	90°	180°	0°	90°	180°	0°	90°	180°
0.25	0.05		1.023	1.033	1.175	1.032	1.040	1.216	1.038	1.045	1.272
	0.1		1.021	1.029	1.116	1.031	1.037	1.144	1.036	1.041	1.179
	0.3		1.017	1.022	1.060	1.024	1.028	1.067	1.028	1.030	1.076
	0.5		1.014	1.016	1.037	1.020	1.022	1.044	1.023	1.023	1.047
0.5	0.05		1.061	1.063	1.349	1.081	1.077	1.361	1.088	1.077	1.382
	0.1		1.050	1.054	1.252	1.074	1.070	1.267	1.082	1.071	1.275
	0.3		1.033	1.031	1.138	1.053	1.048	1.145	1.060	1.051	1.143
	0.5		1.022	1.019	1.085	1.040	1.035	1.095	1.047	1.038	1.096
0.75	0.05		1.098	1.085	1.555	1.130	1.088	1.540	1.137	1.082	1.530
	0.1		1.086	1.073	1.418	1.119	1.080	1.419	1.127	1.075	1.403
	0.3		1.057	1.043	1.191	1.083	1.052	1.215	1.090	1.049	1.212
	0.5		1.043	1.031	1.102	1.062	1.037	1.132	1.068	1.035	1.137

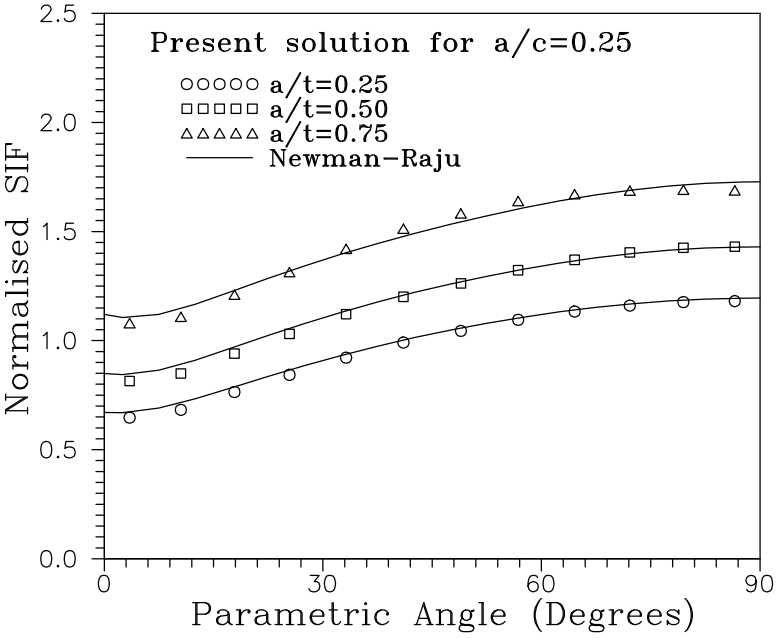

Figure 4: Comparison of SIF solutions for single cracks (a/c=0.25, a/t=0.25-0.75) with Newman-Raju[17]

3.1 Empirical equation for interacting cracks

The interaction factors, γ_B, at location φ=180° evaluated in the present work are fitted by multivariable least square fit in the following form

$$\begin{aligned}\gamma_B =& a_0 + a_1 \ln(\bar{t}_s) + (a_2 + a_3 \ln(\bar{t}_s)) \left(\frac{a}{c}\right) + (a_4 + a_5 \ln(\bar{t}_s)) \left(\frac{a}{c}\right)^2 \\ &+ (a_6 + a_7 \ln(\bar{t}_s)) \left(\frac{a}{t}\right) + (a_8 + a_9 \ln(\bar{t}_s)) \left(\frac{a}{c}\right) \left(\frac{a}{t}\right)\end{aligned} \tag{5}$$

where $\bar{t}_s$ is normalised interspacing i.e. t_s/c

The coefficients a_i evaluated with least square fit are given in Tab. 2. The interaction factors are estimated for interacting cracks from eq.(5) and compared with the numerical values (generated in the present work) in Fig. 8. It is clear from the Fig. 8 that eq. (5) represents the numerical data very accurately.

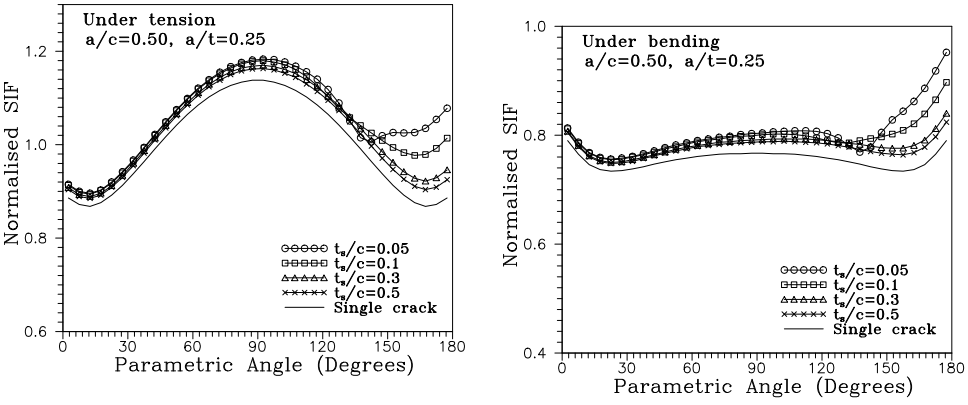

(a) (b)

Figure 5: (a) Normalised stress intensity factor in mode-I for multiple in-plane semi-elliptical cracks (a/c=0.5) in a finite solid (a/t= 0.25, c/W=0.20) under tension, (b) Normalised stress intensity factor in mode-I for multiple in-plane semi-elliptical cracks (a/c=0.5) in a finite solid (a/t= 0.25, c/W=0.20) under bending

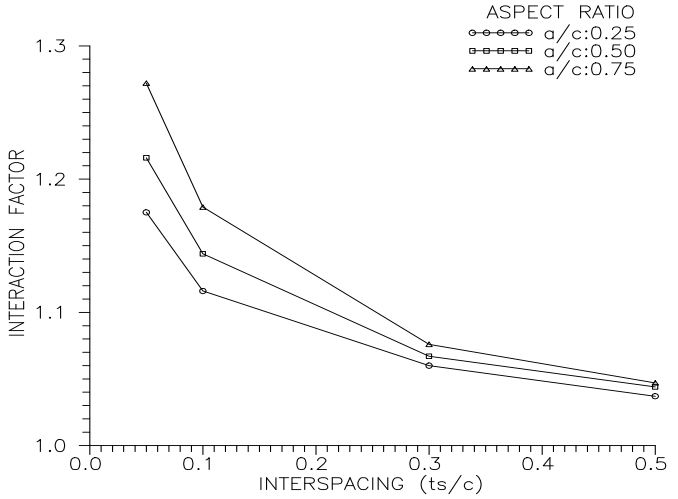

Figure 6: Effect of cracks interspacing (t_s/c) and aspect ratio (a/c) on interaction factor under uniform tension (a/t=0.25)

3.2 Multiple Coalescing Surface Cracks

Here, the improved modified virtual crack closure integral method is used to obtain the stress intensity factor solutions for a wide variety of parameters of coalescing

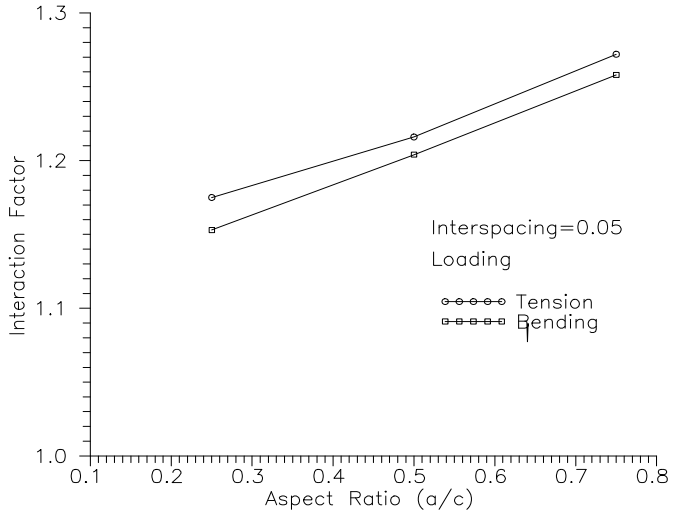

Figure 7: Effect of type of loading on interaction factor

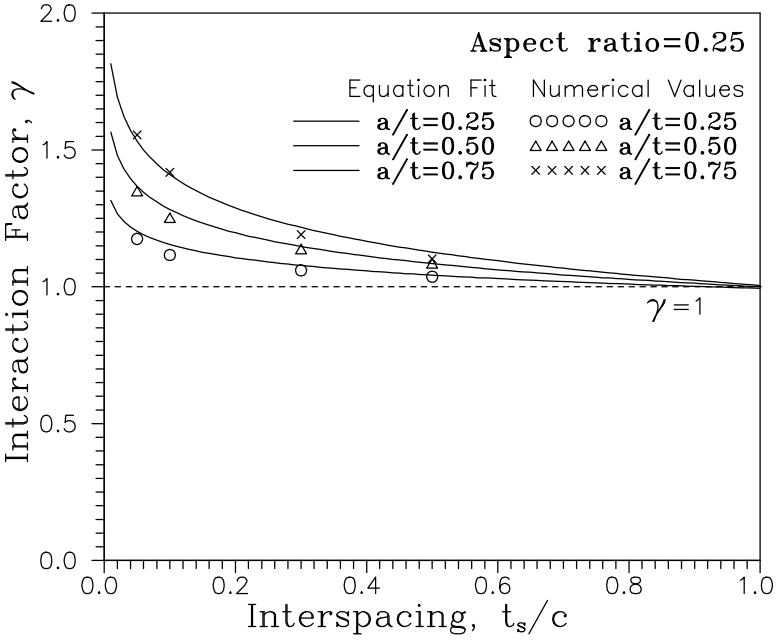

Figure 8: Correlation between eq.(5) for interaction factors and numerical data

Table 2: Coefficients a_i in eq. (5).

a_0=1.013815113	a_1=0.0391813193	a_2=0.03512327218	a_3=-0.07534944455
a_4=-0.1699475003	a_5=-0.07223897935	a_6=-0.1316018562	a_7=-0.3447194355
a_8=0.3061928307	a_9=0.2647192415		

coplanar equal semi-elliptical cracks subjected to tension loading. Since the interaction factor is only marginally dependent on the type of loading (as clear from discussion of previous section), the interaction factor for coalescing cracks subjected to bending load is not considered. The definition of geometric parameters of coalescing crack configuration is given in Fig. 9.

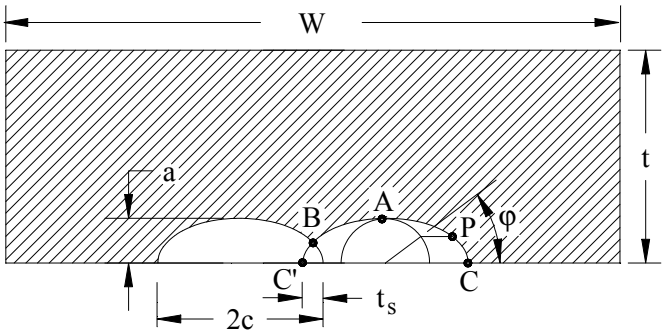

Figure 9: Definition of geometric parameters of coalescing crack configuration

Following crack configurations (total 54 cases) in a wide body (c/W=0.2) are considered in the present study:

Aspect Ratio (a/c) = 0.25, 0.50 and 0.75

Thickness Ratio (a/t) = 0.25, 0.50 and 0.75

Interspacing (t_s/c) = -0.01, -0.03, -0.05, -0.1, -0.3 and -0.5.

One of the finite element models of coalescing cracks (a/c=0.5, a/t=0.5, t_s/c=-0.05) is shown in Fig. 10. This is also for half the domain considering two equal coalescing cracks. The models consist of degrees of freedom varying from 8712-11946. The definition of interaction factor (γ) is same as described in the previous section.

The variation of normalised stress intensity factor along the crack front at aspect ratio of a/t=0.25 and a/c=0.25 is depicted in Fig. 11(a) and similarly same for a/t=0.25 and a/c=0.5 is shown in Fig. 11(b). The parameter varying across these curves is

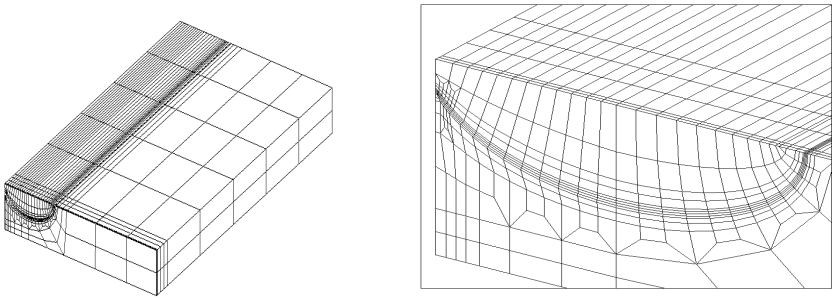

(a) **(b)**

Figure 10: (a) Finite element model of coalescing cracks (a/c=0.5, a/t=0.5, t_s/c=-0.05). (b) Details of mesh at crack tip

interspacing t_s/c. It is observed that the SIF is principally influenced in region close to coalescence region, within 30-60 degrees from the coalescing plane. The SIF at this plane increases with aspect ratio and this is true for any interspacing. The SIF at coalescence plane with respect to interspacing ratio does not show any clear trend. For example, in case of configuration with a/t=0.25 and a/c=0.25 (Fig. 11(a)), the SIF at this plane first decreases with interspacing ratio upto t_s/c=-0.05 then found to be increasing with increasing absolute value of t_s/c. Whereas for configuration with a/t=0.25 and a/c=0.50 (Fig. 11(b)), the SIF at this plane reduces with increase in absolute value of interspacing. Soboyejo et al. [Soboyejo, Knott, Walse and Cropper (1990)] defined the interaction factor as the ratio of stress intensity factor at coalescence plane (location 'B') to that of SIF at location 'C' in case of single crack. However, for locations A and C the interaction factor was evaluated as the ratio of SIF at the same location with and without neighboring crack.

The variation of interaction factor γ_B with interspacing for various aspect ratios is shown in Fig. 12. For all the cases except a/c=0.25 the interaction factor reduces with increase in interspacing distance i.e. during crack coalescence the stress intensity factor is maximum at the beginning of coalescence. The interaction factor of a/c=0.25 first decreases for increase in interspacing (upto t_s/c=-0.05) but thereafter it increases with interspacing. This happens since the interaction factor is defined relative to SIF at point 'C' i.e. at parametric angle φ=180°. But as it is observed that the stress intensity factor is a function of parametric angle for elliptical crack, the base SIF (of point 'C') used for evaluation of interaction factor (as used by Soboyejo[Soboyejo, Knott, Walse and Cropper (1990)]) does not provide true estimate of amplification on SIF. Thus logically speaking, the interaction factor should

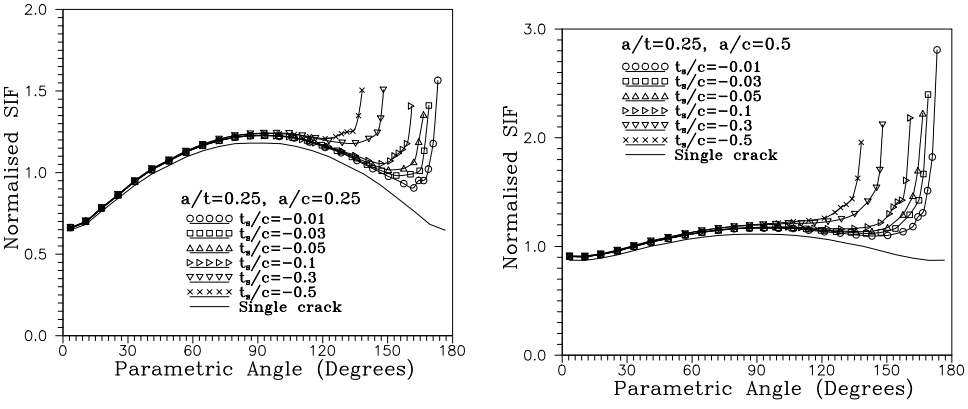

(a) (b)

Figure 11: (a) Variation of SIF distribution for coalescing semi-elliptical cracks (a/t=0.25, a/c=0.25) with crack separation distance (t_s/c). (b) Variation of SIF distribution for coalescing semi-elliptical cracks (a/t=0.25, a/c=0.50) with crack separation distance (t_s/c)

be defined based on SIF of single crack in same body at the same parametric angle of coalescing plane. We call this as absolute interaction factor and this is plotted with interspacing for various aspect ratios in Fig. 13 (a)-(c). It is evident from Fig. 13 (a)-(c) that the behavior of absolute interaction factor is monotonic at coalescing plane.

It is also observed that the interaction factor is a strong function of aspect ratio and thickness ratio, and increases with increase in both the parameters. For locations 'A' and 'C' the interaction factors are found to be small compared to point 'B'. The absolute interaction factors for various aspect ratios, thickness ratios and interspacing are given in Tab. 3 which can directly be used for crack growth simulation.

3.3 Empirical equation for coalescing cracks

It can be observed form the results of coalescing cracks that the interaction factor at a location is a function of interspacing (t_s), aspect ratio (a/c) and thickness ratio (a/t). Thus, first least square fit technique is applied and interaction factor was obtained as a function of thickness and aspect ratios. Subsequently, effect of interspacing is accounted for by another parametric equation. The interaction factor for

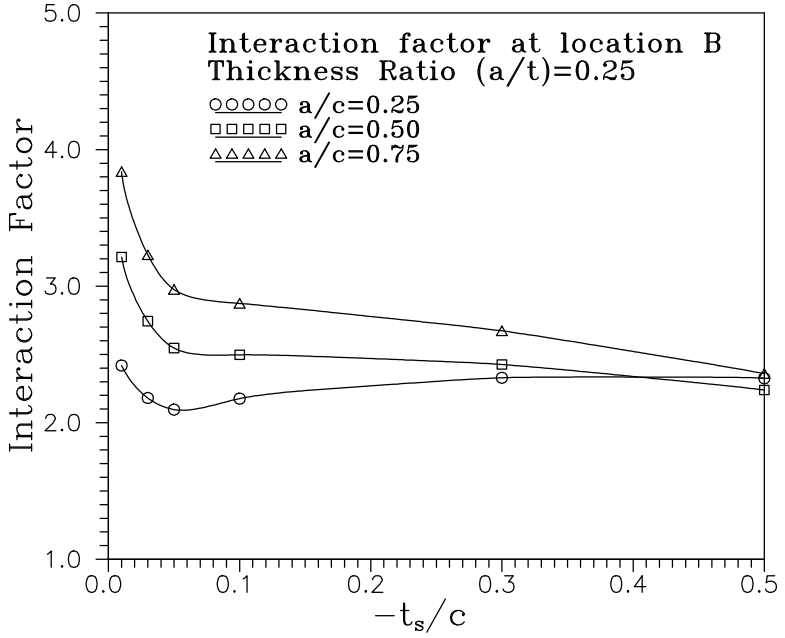

Figure 12: Interaction factors for coalescing cracks for various values of aspect ratio for thickness ratio (a/t)=0.25

coalescing crack at location 'B' is written as

$$\gamma_B = f_{ts} g \left[b_0 + b_1 \left(\frac{a}{c}\right) + b_2 \left(\frac{a}{t}\right) + b_3 \left(\frac{a}{c}\right)\left(\frac{a}{t}\right) + b_4 \left(\frac{a}{c}\right)^2 \left(\frac{a}{t}\right) + b_5 \left(\frac{a}{c}\right)\left(\frac{a}{t}\right)^2 + b_6 \left(\frac{a}{c}\right)^2 \left(\frac{a}{t}\right)^2 \right] \quad (6)$$

where g is a 'fine tune' parameter which should have a limiting values of interaction factor (γ=1) for various aspect ratios and thickness ratios at $\bar{t}_s$=2 (represents single crack) given as

$$g = 1 - 0.12\left(\frac{a}{t} - 0.25\right)(\bar{t}_s)^p \left\{ 1 + 0.3\left(\frac{a}{c}\right)\left(\frac{a}{t}\right) - 0.6\left(\frac{a}{c}\right)^2 \left(\frac{a}{t}\right)^2 \right\}$$

where $p = 1 + \frac{a}{c} + \frac{a}{t}$.

It was observed that the interaction factor changes rapidly with t_s upto $\bar{t}_s$=0.1, subsequently, its variation is nearly linear. Thus, the least square fit has been separated

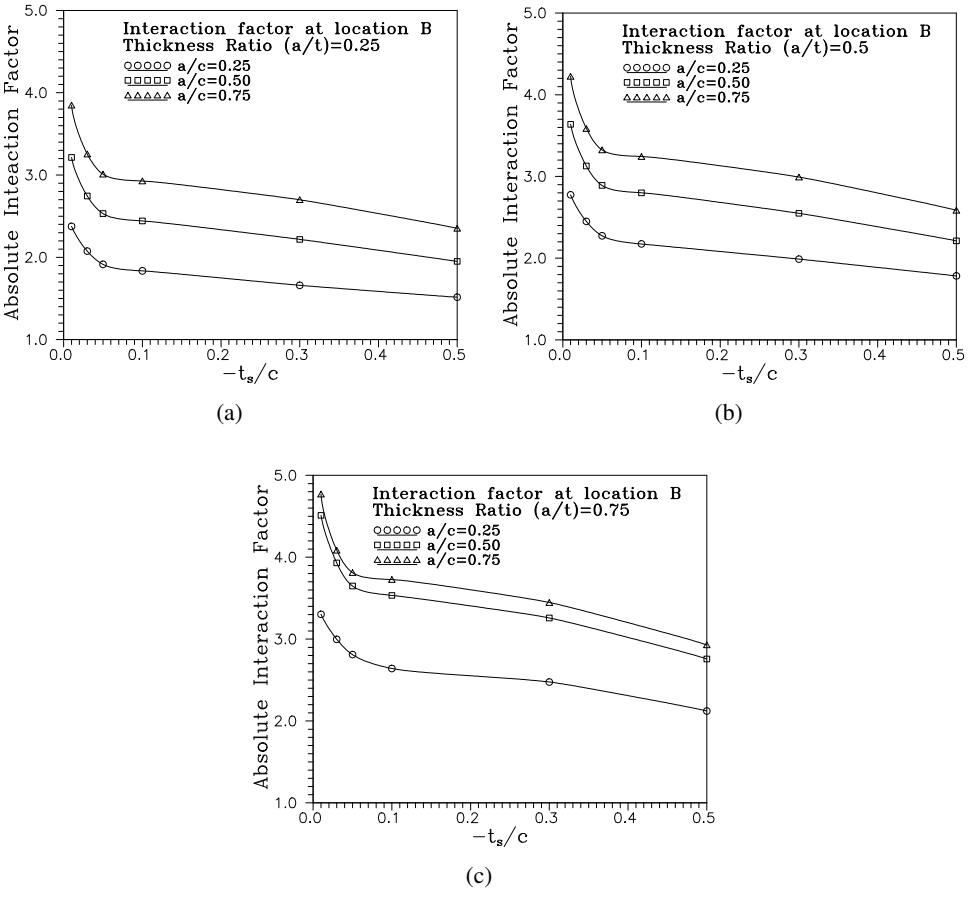

Figure 13: (a) Absolute interaction factors for coalescing cracks for various values of aspect ratio for thickness ratio (a/t)=0.25. (b) Absolute interaction factors for coalescing cracks for various values of aspect ratio for thickness ratio (a/t)=0.5. (c) Absolute interaction factors for coalescing cracks for various values of aspect ratio for thickness ratio (a/t)=0.75

in two parts. The first part is valid upto $\bar{t}_s$<0.1 and fitted with fourth order polynomial whereas the second part is valid in the range of $\bar{t}_s$=0.1 to 2.0 and fitted with second order polynomial. It can be observed, the definition of interaction factor that the interaction approaches to unity at all locations (A, B and C) as $\bar{t}_s$ approaches 2. Thus, this limiting value of γ_B equal to 1.0 is used at $\bar{t}_s$=2.0 at various aspect ratios of cracks. The effect of thickness on the interaction factor is accounted for by the

Table 3: Absolute interaction factors at positions B, A, and C.

a/c	t_s/c	a/t =0.25			a/t=0.50			a/t=0.75		
		γ_B	$\gamma_{A(90)}$	$\gamma_{C(0)}$	γ_B	γ_A	γ_C	γ_B	γ_A	γ_C
0.25	-0.01	2.376	1.039	1.025	2.775	1.075	1.053	3.302	1.085	1.070
	-0.03	2.075	1.038	1.023	2.450	1.079	1.056	2.997	1.098	1.095
	-0.05	1.914	1.040	1.023	2.274	1.085	1.060	2.811	1.107	1.105
	-0.10	1.835	1.037	1.022	2.174	1.085	1.058	2.641	1.103	1.094
	-0.30	1.660	1.050	1.028	1.989	1.110	1.075	2.476	1.154	1.142
	-0.50	1.515	1.048	1.020	1.783	1.114	1.071	2.122	1.159	1.127
0.50	-0.01	3.214	1.049	1.039	3.638	1.095	1.091	4.511	1.190	1.228
	-0.03	2.745	1.052	1.040	3.128	1.101	1.097	3.930	1.200	1.246
	-0.05	2.531	1.054	1.040	2.890	1.106	1.101	3.648	1.209	1.254
	-0.10	2.442	1.057	1.040	2.800	1.115	1.107	3.534	1.222	1.265
	-0.30	2.218	1.075	1.047	2.549	1.148	1.130	3.258	1.264	1.326
	-0.50	1.950	1.082	1.041	2.212	1.160	1.132	2.758	1.296	1.321
0.75	-0.01	3.849	1.061	1.047	4.225	1.100	1.109	4.771	1.103	1.174
	-0.03	3.255	1.066	1.049	3.586	1.109	1.116	4.085	1.115	1.190
	-0.05	3.010	1.068	1.051	3.325	1.115	1.121	3.812	1.122	1.202
	-0.10	2.927	1.076	1.051	3.244	1.129	1.132	3.727	1.140	1.222
	-0.30	2.699	1.104	1.061	2.993	1.165	1.156	3.447	1.189	1.269
	-0.50	2.352	1.115	1.058	2.586	1.183	1.161	2.929	1.213	1.273

terms in the bracket of eq.(6) and the effect of interspacing ($\bar{t}_s$) is represented as follows:

$$f_{ts} = \left(a_0 + a_1\bar{t}_s^{+}a_2\bar{t}_s^2 + a_3\bar{t}_s^3 + a_4\bar{t}_s^4\right) + \left(a_5 + a_6\bar{t}_s^{+}a_7\bar{t}_s^2 + a_8\bar{t}_s^3 + a_9\bar{t}_s^4\right)\left(\frac{a}{c}\right) + \left(a_{10} + a_{11}\bar{t}_s^{+}a_{12}\bar{t}_s^2 + a_{13}\bar{t}_s^3 + a_{14}\bar{t}_s^4\right)\left(\frac{a}{c}\right)^2$$

For $\bar{t}_s$<0.1.

and

$$f_{ts} = \left(a_{15} + a_{16}\bar{t}_s^{+}a_{17}\bar{t}_s^2\right) + \left(a_{18} + a_{19}\bar{t}_s^{+}a_{20}\bar{t}_s^2\right)\left(\frac{a}{c}\right) + \left(a_{21} + a_{22}\bar{t}_s^{+}a_{23}\bar{t}_s^2\right)\left(\frac{a}{c}\right)^2 \quad (7)$$

For $0.1 \leq \bar{t}_s \leq 2$.

where positive and normalized value of interspacing i.e. $\bar{t}_s$ has been considered. The coefficients in eq.(6) are determined for locations 'B' and given in Tab. 4. Eq.(6) is generally accurate within 2%, however, at the limiting values of interspacing, $\bar{t}_s$, (equal to 2) the error is found to be within 6%.

Table 4: Coefficients for location 'B' in eq.(6).

Coefficients a_i

a_0=1.450189381	a_1=-12.55647713	a_2=205.9764320	a_3=-1444.376452
a_4=2938.526285	a_5=5.003239267	a_6=-49.7539799	a_7=220.0115025
a_8=1546.596142	a_9=-6042.25784	a_{10}=-1.526420392	a_{11}=-13.33773731
a_{12}=840.5565687	a_{13}=-8487.303625	a_{14}=19557.89619	a_{15}=1.148717900
a_{16}=-0.3174026763	a_{17}=0.1217113293	a_{18}=3.502034045	a_{19}=-3.372128914
a_{20}=0.8100193548	a_{21}=-1.211662752	a_{22}=2.300021769	a_{23}=-0.8470418449

Coefficients b_i

b_0=0.91505583	b_1=0.07219005	B_2=0.48590438	
b_3=-2.03341992	b_4=1.83890792	B_5=4.33947915	B_6=-4.80896730

The interaction factors are estimated from eq.(6) for various thickness ratios and interspacings for coalescing cracks and compared with numerical values (Tab. 2) in Fig. 14. It is clear from the Fig. 14 that eq. (6) represents the numerical data very accurately.

4 Concluding Remarks

Improved MVCCI technique was utilized to study the interaction effects between two surface cracks in a finite body under uniform tension and pure bending. The study is of great significance for problems of multisite damage in aging structures. The effect of geometric parameters on the interaction factor is presented. It is found that the interaction factor significantly increases with aspect ratio but the type of loading i.e. tension or bending has marginal effect on the interaction factor. As expected, the results also indicate that the interaction effect is significant when the cracks are separated by a small distance. As the distance between two cracks is increased to approximately equal to the length of a crack (t_s/c=0.5), the interaction factor is negligible.

The numerically evaluated stress intensity factors are also presented for coalescing phase of multiple cracks. For coalescing cracks the interaction factor as defined earlier by Soboyejo et al [Soboyejo, Knott, Walse and Cropper (1990)] does not provide a clear picture of behavior of coalescing cracks with respect to interspacing. Thus a different definition of interaction factor called absolute interaction factor

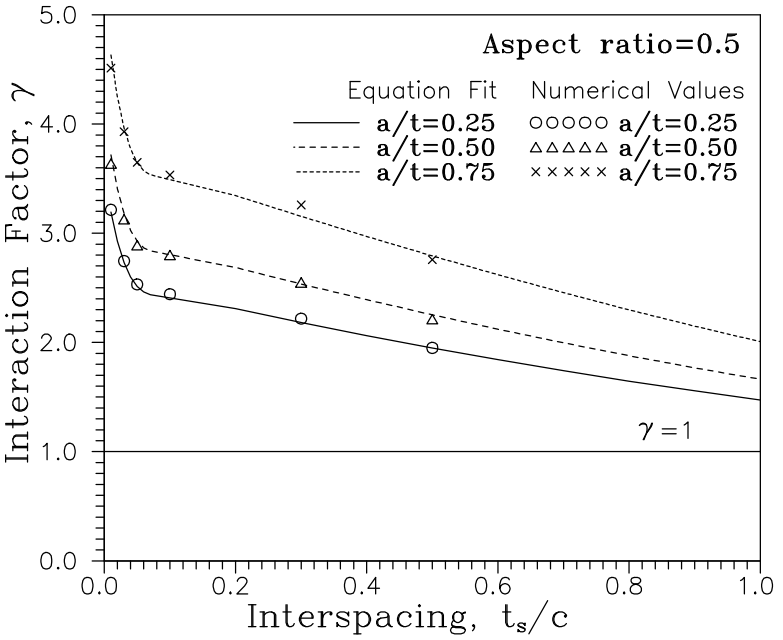

Figure 14: Variation of interaction factor with interspacing, a comparison between the numerical values and eq. (6)

is proposed. It is demonstrated that the absolute interaction factor explains the behavior of coalescing cracks in a better way. The absolute interaction factor is found to be a monotonic function of interspacing. It is also observed in coalescing phase too that the interaction factor increases with the thickness ratio and aspect ratio. This clearly shows that the interaction factor of multiple cracks in infinite body can not directly be used in life prediction of finite (real) bodies.

Using the finite element estimates of interaction factors for twin coplanar semi-elliptical cracks, empirical equations are formulated for interacting and coalescing cracks to facilitate their direct use in the fatigue crack growth simulation and crack shape mapping of multiple cracks in a finite body.

References

Badari Narayana, K.; Dattaguru, B.; Ramamurthy, T. S.; Vijaykumar, K. (1994): *A general procedure for modified crack closure integral in 3-d problems with cracks*, Eng. Fract. Mech. 48, 194, pp. 167-176.

Buchholz, F. G. (1984): Improved formulae for the FE-calculation of the strain

energy release rate by the modified crack closure integral method, *Proc. 4th World Congress and Exhibit on the Finite Element Methods, Interlaken*, pp. 650-659.

Chahardehi, A.; Brennan, F. P.; Han, S. K. (2010): Surface crack shape evolution modeling using an RMS SIF approach, *Int. J. Fatigue*, 32, pp. 297-301.

Donoghue, P. E.; Nishioka, T.; Atluri, S. N. (1986): Analysis of interaction behavior of surface flaws in pressure vessel, *J. Press. Vess. Tech. ASME* 108, pp. 24-32.

Isida, M.; Yoshida, T.; Naguch. H. (1990): A finite thickness plate with a pair of semi-elliptical surface cracks, *Eng. Fract. Mech.*, 35, pp. 961-965.

Kamaya, M. (2008): Growth evaluation of multiple interacting surface cracks, *Part I: Experiments and coalesced crack*, 75, pp. 1336-1349. Part II: Growth evaluation of parallel cracks, Eng. Fract. Mech., 75, pp. 1350-1366.

Kishimoto, K.; Soboyejo, W. O.; Smith, R.A.; Knott, J. F. (1989): A numerical investigation of the interaction and coalescence of two coplanar semi-elliptical cracks, *Int. J of Fat.*, 11, pp. 91-96.

Kruger, R. (2004): Virtual crack closure technique: History, approach and applications, *Applied Mechanics Reviews*, 57, pp. 109-143.

Lin, X. B.; Smith, R. A. (1999): Finite element modeling of fatigue crack growth of surface cracked plates, *Part II: Crack shape change, Engng. Fract. Mech.*, 63, pp. 523-540 and Part III: Stress Intensity factor and fatigue crack growth life, *Engng. Fract. Mech.*, 63, pp. 541-556.

Murakami, Y.; Nemat-Nasser, S. (1982): Interacting dissimilar semi-elliptical surface flaws under tension and bending, *Eng. Fract. Mech.*, 16, pp. 373-386.

Narayana, K. B.; George, S.; Dattaguru, B.; Ramamurthy, T. S.; Vijaykumar, K. (1994): Modified crack closure integral for 3-D problems using 20-noded brick elements, *Fat. Eng. Mater. Struct*., 17, pp. 145-157.

Newman, J. C. Jr.; Raju, I. S. (1979): Analyses of surface cracks in finite plates under tension or bending loads, *NASA TP* 1578.

Newman, J. C. Jr.; Raju, I. S. (1981): An empirical stress intensity factor equation for the surface flaw, *Eng. Fract. Mech.*, 15, pp. 185-192.

Patel, S. K. (2000): Experimental and Numerical studies on Fatigue crack growth of single and interacting multiple surface cracks, *Ph.D. Thesis, Indian Institute of Science, Bangalore, India.*

Rybicki, E. F.; Kanninen, F. M. (1977): A finite element calculation of stress intensity factors by modified crack closure integral, *Eng. Fract. Mech.*, 9, pp. 931-938.

Soboyejo, W. O.; Knott, J. F.; Walse, M. J.; Cropper, K. R. (1990): Fatigue crack-propagation of coplanar semi-elliptical cracks in pure bending, *Eng. Fract. Mech.*, 37, pp. 323-340.

Xiao, X; Yan, X. (2007): A new numerical analysis for a semi-circular surface crack, *Eng. Fract.Mech.*, 74, pp. 2639-2641.